JIPF (JURNAL ILMU PENDIDIKAN FISIKA)
p-ISSN: 2477-5959 | e-ISSN: 2477-8451 *Vol. 9 No. 1, January 2024, Page 135-141*

Determination of Wavelength of He-Ne Laser and Diode Laser Using Single Slit Diffraction Method

Sri Purwaningsih [1], Hebat Shidow Falah [2*)], Neneng Lestari [3], Dwi Sartika Sari [4], Edi Yuversa [5]
Universitas Jambi, Indonesia[1,2,3,4,5]
[*)]Corresponding E-mail: hebatshidowfalah@unja.ac.id

Received: October 7th, 2023. Revised: November 8th, 2023. Accepted: November 15th, 2023

Keywords :
Diffraction; Single Slit Experiment, He-Ne Laser; Diode Laser

ABSTRACT
This research aims to investigate/determine the value of the laser wavelength produced by He-Ne lasers and Diode lasers using the concept of diffraction at a single slit. The gaps used consist of three types of gaps which have gaps with a width of 0.12 mm, 0.24 mm, and 0.48 mm. Experimental results show that the wavelength of He-Ne laser light ranges from 640 nm to 646 nm. Meanwhile, the wavelength of He-Ne laser light ranges from 640 nm to 686.67 nm. Based on the results obtained, it can be concluded that it is proven that the wavelength calculated using the single slit diffraction method is in the range of values for lasers that emit red light.

INTRODUCTION

Diffraction is a physical phenomenon that can be explained using concepts in modern physics. In the phenomenon of diffraction, light is seen and behaves as a wave [1] [2] [3]. When passing through a thin slit, the light that passes through the slit has unique properties, it can form a light-dark pattern [4] [5]. The distance of the light-dark pattern (y) is influenced by the width of the slit (d), the distance between the slit and the screen (L), and the wavelength of the light that hits it (λ). The concept of this phenomenon is explained through the relation

$$d \sin\theta = n\lambda; \qquad n = 1,2,3,\ldots \tag{1}$$

with n being the order of minimum intensity. Because the distance between the slit and the screen is much greater than the slit width, then $y \approx r$ so the value of $\sin\theta = y/L$. Thus, the equation (1) becomes

$$d\frac{y}{L} = n\lambda \tag{2}$$

A schematic of the diffraction phenomenon can be seen in Figure 1.

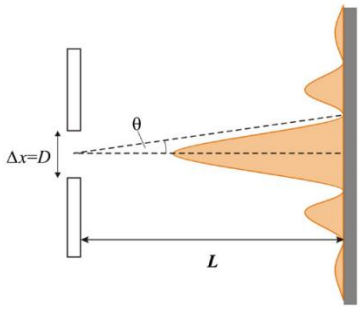

***Fig 1**. Single-slit diffraction experiment* [6]

Because it has these properties, lasers are often used as light sources in various fields, such as in the fields of education, research, and applications in the health sector, etc [7] [8] [9] [10] [11] [12] [13]. Based on its energy density, coherence, and direction, lasers have been widely applied in applied fields throughout the world in the fields of materials [14] [15], surface treatment on laser surface alloys [16], laser remelting [17] [18] [19] and so on [20]. In the field of education and simple experiments, lasers are often used in experimental activities, such as light reflection properties, light refraction properties, light diffraction, etc [21] [22] [23] [24] [25] [26]. There are two types of lasers that are often used in education and research: diode lasers and He-Ne lasers.

Laser diodes are the main optical sources in various optical fibers and are indispensable for our daily lives [27]. Diode lasers are widely applied in the field of education [24]. Historically, Helium-Neon (He-Ne) lasers have often been the primary choice for precision measurement instruments, measurement devices, and some spectroscopic applications. The He-Ne laser was initiated in 1960 and was the first laser to have extraordinary parameters.

He-Ne lasers have been widely researched and developed so that they have become a type of laser that has frequency stabilization and high performance [28] [29] [30]. The use of He-Ne lasers has several advantages over other types of lasers: high coherence length, stable central wavelength, high spectral purity, high beam quality and alignment, and low cost. However, the use of He-Ne lasers also has disadvantages: short lifetime, long warm-up time, low output power, very bulky, and consumes high voltage.

METHOD

This research is an experimental research method. Tools and materials used in the experiment are: He-Ne Laser (linear polarized), laser diode, holder with spring clip, diaphragm (469 91) optical lens (f=+5mm and f=+55mm), precision rail, 4 rider optics, screens, saddle base. The experimental setup is shown in Figure 2.

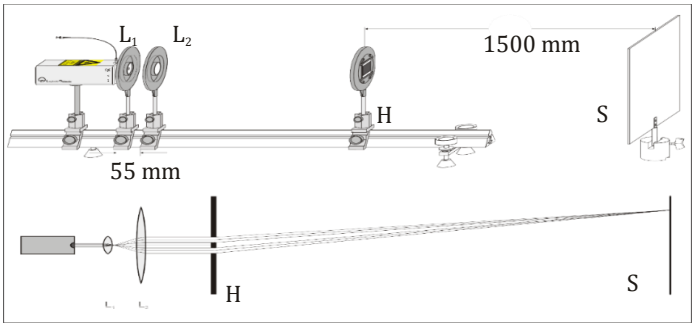

***Fig 2.** Experimental setup in single-slit diffraction*

The first lens ($f = +5\ mm$) is placed near the laser as a light source. The second lens with $f = +50$ mm is placed 55 mm away from the first lens. This placement is adjusted in such a way that the light that passing through the second lens is parallel. The light that comes out of this lens then hits the diaphragm which diffracts the light. The screen is placed 1500 mm behind the diaphragm as a tool to capture the light pattern formed after the light is diffracted.

The light emitted by the He-Ne laser and diode laser will hit the positive lens (f=5 and f=55mm). This aims to expand the cross-section of the laser beam produced by the laser. The lens position is adjusted so that even though the beam's cross-section is enlarged, the resulting rays remain parallel. This expanded beam then hits the diaphragm with three different gap distances, namely 0.12 mm, 0.24 mm, and 0.48 mm. After hitting the diaphragm, the diffraction pattern through a single slit using a He-Ne laser and a diode laser is visible as a pattern on the screen as shown in Figures 3 and 4.

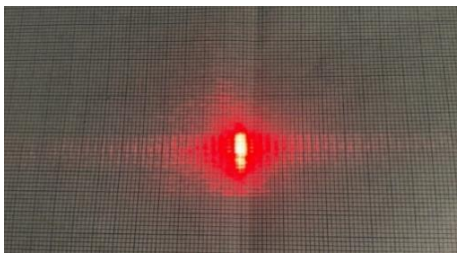

Fig 3. *Light diffraction pattern using a He-Ne laser*

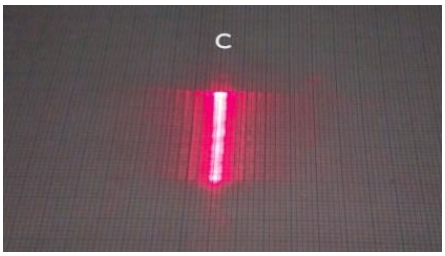

Fig 4. *Light diffraction pattern using a Diode laser*

RESULTS AND DISCUSSIONS

Two different lasers (He-Ne and Diode) were used to calculate the wavelength based on the pattern that appears in the diffraction phenomenon. On each laser, diffraction experiments were carried out using a single slit diaphragm. Each laser will be experimented with three treatment parameters, namely gaps with a width of 0.12 mm, 0.24 mm, and 0.48 mm. The data taken is data on the distance (y_n) of the first ($n = 1$), second ($n = 2$), and third ($n = 3$) dark patterns from the center point of the diffraction pattern. This data is then used to calculate the diffracted wavelength value using the equation

$$\lambda = dyn^{-1}L^{-1} \tag{1}$$

with n being the n-th minimum intensity order formed on the screen.

The experiment data to obtain the wavelength of the He-Ne laser is presented in Table 1.

Table 1. He-Ne laser wavelength

d(mm)	L(mm)	y1(mm) y2(mm) y3(mm)	λ (nm)	Average (nm)
0.12	1500	9	720	686.67
		17	680	
		25	660	
0.24	1500	5	640	666.67
		9	720	
		12	640	
0.48	1500	3	640	640
		5	640	
		7	640	

The measurement results produce a distance value of the first (minimum) dark pattern (y_1) of 9 mm from the central light from a light that passes through a single slit of 0.12 mm. Using equation (3), a wavelength value of 720 nm is obtained. The second dark pattern measurement (y_2) is 17 mm from the central light, with a calculated wavelength value of 680 nm. The measurement of the third dark pattern (y_3) is 25 mm from the central light, with a calculated wavelength value of 660 nm. Based on the calculated values of the three wavelengths, an average laser wavelength value of 686.67 nm was obtained.

Using a single slit d = 0.24 mm and a screen distance of 1.5 m, the distance of the first dark pattern (y_1) is 5 mm from the central light. This is logical because based on equation (2), the wider the gap used, the denser the resulting pattern. The second dark pattern measurement (y_2) is 9 mm from the central light, with a calculated wavelength value of 720 nm. The measurement of the third dark pattern (y_3) is 12 mm from the central light, with a calculated wavelength value of 640 nm. Based on the calculated values of the three wavelengths, an average laser wavelength value of 666.67 nm was obtained.

Using a single slit d = 0.48 mm and a screen distance of 1.5 m, the distances of the first (y_1), second (y_2), and third (y_3) dark patterns become denser: 3 mm, 5 mm, and 7 mm, respectively. using equation (3), a similar result is obtained, namely 640 nm. This shows that the wider the gap used, the tighter the pattern formed, in accordance with equation (2). A further conclusion is that based on the results of measurements and calculations, the average values of the measured He-Ne laser wavelengths are in accordance with [31] [32] [33].

Table 2. Diode laser wavelength

d(mm)	L(mm)	y1(mm) y2(mm) y3(mm)	λ (nm)	Average (nm)
0.12	1500	9	720	673.33
		16	640	
		25	660	
0.24	1500	4	640	640
		8	640	
		12	640	
0.48	1500	3	640	640
		5	640	
		7	640	

Table 2 shows the results of wavelength measurements for diode lasers. We found that a gap of d = 0.12 mm and a screen distance of 1.5 m resulted in a distance of the first (minimum) dark pattern (y_1)

of 9 mm from the central light. Using equation (3), a wavelength value of 720 nm is obtained. The second dark pattern measurement (y_2) is 16 mm from the central light, with a calculated wavelength value of 640 nm. The measurement of the third dark pattern (y_3) is 25 mm from the central light, with a calculated wavelength value of 660 nm. Based on the calculated values of the three wavelengths, an average laser wavelength value of 673.33 nm was obtained.

Using a single slit d = 0.24 mm and a screen distance of 1.5 m, the distance of the first dark pattern (y_1) is 4 mm from the central light and produces a calculated wavelength value of 640 nm. The second dark pattern measurement (y_2) is 8 mm from the central light, and the calculated wavelength value is 640 nm. The measurement of the third dark pattern (y_3) is 12 mm from the central light, and the calculated wavelength value is 640 nm. Based on the calculated values of the three wavelengths, an average laser wavelength value of 640 nm is obtained.

Using a single slit d = 0.48 mm and a screen distance of 1.5 m, the distances of the first (y_1), second (y_2), and third (y_3) dark patterns become denser, namely 3 mm, 5 mm, and 7 mm, respectively. The calculation results obtained the same wavelength, namely 640 nm.

Through experiments using a He-Ne laser and a Diode laser, results were obtained that were not much different. The range of wavelength values obtained through experiments is in the range of values from 640 nm to 686.67 nm. This indicates that this experiment is still in accordance with the reference which states that the laser wavelength with red visible light is in the range of 630 nm to 700 nm [34] [35] [36] [37].

CONCLUSION AND SUGGESTION

Based on the experiments that have been carried out, it can be concluded that the wavelength produced by the He-Ne laser with red light is in the range of 640 nm to 686.67 nm. Meanwhile, the wavelength produced by a diode laser with red light is in the range of 640 nm to 673.33 nm. This study used a single diffraction slit with slit widths of 0.12 mm, 0.24 mm and 0.48 mm. These results are in accordance with the literature which states that lasers with red light have a wavelength between 630 nm and 700 nm.

ACKNOWLEDGMENTS

The author thanks the Faculty of Teacher Training and Education, Jambi University, which has provided funding for this research. We would also like to thank the physics education study program for allowing the author to carry out experimental activities in the basic physics education laboratory.

REFERENCES

[1] Yoon, J. W., Kim, Y. G., Choi, I. W., Sung, J. H., Lee, H. W., Lee, S. K., & Nam, C. H. (2021). Realization of laser intensity over 10 23 W/cm 2. *Optica*, *8*(5), 630-635.
[2] Collini, M., D'Alfonso, L., & Chirico, G. (2016). Hands-on Fourier analysis by means of far-field diffraction. *European Journal of Physics*, *37*(6), 065701.
[3] Gates-Rector, S., & Blanton, T. (2019). The powder diffraction file: a quality materials characterization database. *Powder Diffraction*, *34*(4), 352-360.
[4] Rivera-Ortega, U., & Pico-Gonzalez, B. (2015). Wavelength estimation by using the Airy disk from a diffraction pattern with didactic purposes. *Physics Education*, *51*(1), 015012.
[5] Gemmi, M., Mugnaioli, E., Gorelik, T. E., Kolb, U., Palatinus, L., Boullay, P., ... & Abrahams, J. P. (2019). 3D electron diffraction: the nanocrystallography revolution. *ACS Central Science*, *5*(8), 1315-1329.

[6] Nikolic, D., & Nesic, L. (2011). Verification of the uncertainty principle by using diffraction of light waves. *European journal of physics*, *32*(2), 467.
[7] Passarella, S., Casamassima, E., Molinari, S., Pastore, D., Quagliariello, E., Catalano, I. M., & Cingolani, A. (1984). Increase of proton electrochemical potential and ATP synthesis in rat liver mitochondria irradiated in vitro by helium-neon laser. *FEBS letters*, *175*(1), 95-99.
[8] Van Breugel, H. H., & Bär, P. D. (1992). Power density and exposure time of He-Ne laser irradiation are more important than total energy dose in photo-biomodulation of human fibroblasts in vitro. *Lasers in surgery and medicine*, *12*(5), 528-537.
[9] Hawkins, D. H., & Abrahamse, H. (2006). The role of laser fluence in cell viability, proliferation, and membrane integrity of wounded human skin fibroblasts following helium-neon laser irradiation. *Lasers in Surgery and Medicine: The Official Journal of the American Society for Laser Medicine and Surgery*, *38*(1), 74-83.
[10] Bensadoun, R. J., Franquin, J. C., Ciais, G., Darcourt, V., Schubert, M. M., Viot, M., ... & Demard, F. (1999). Low-energy He/Ne laser in the prevention of radiation-induced mucositis: A multicenter phase III randomized study in patients with head and neck cancer. *Supportive care in cancer*, *7*, 244-252.
[11] Lyons, R. F., Abergel, R. P., White, R. A., Dwyer, R. M., Castel, J. C., & Uitto, J. (1987). Biostimulation of wound healing in vivo by a helium-neon laser. *Annals of plastic surgery*, *18*(1), 47-50.
[12] Hu, W. P., Wang, J. J., Yu, C. L., Lan, C. C. E., Chen, G. S., & Yu, H. S. (2007). Helium–neon laser irradiation stimulates cell proliferation through photostimulatory effects in mitochondria. *Journal of Investigative Dermatology*, *127*(8), 2048-2057.
[13] Roberts III, T. L., & Yokoo, K. M. (1998). In pursuit of optimal periorbital rejuvenation: laser resurfacing with or without blepharoplasty and brow lift. *Aesthetic Surgery Journal*, *18*(5), 321-332.
[14] Leech, P. W. (2014). Laser surface melting of a complex high alloy steel. *Materials & Design (1980-2015)*, *54*, 539-543.
[15] Ahmadi-Pidani, R., Shoja-Razavi, R., Mozafarinia, R., & Jamali, H. (2014). Improving the hot corrosion resistance of plasma sprayed ceria–yttria stabilized zirconia thermal barrier coatings by laser surface treatment. *Materials & Design*, *57*, 336-341.
[16] Nair, A. M., Muvvala, G., & Nath, A. K. (2019). A study on in-situ synthesis of TiCN metal matrix composite coating on Ti–6Al–4V by laser surface alloying process. *Journal of Alloys and Compounds*, *810*, 151901.
[17] Wang, Z., Zhang, Q., Bagheri, R., Guo, P., Yao, Y., Yang, L., & Song, Z. (2019). Influence of laser surface remelting on microstructure and degradation mechanism in simulated body fluid of Zn-0.5 Zr alloy. *Journal of Materials Science & Technology*, *35*(11), 2705-2713.
[18] Soleimanipour, Z., Baghshahi, S., & Shoja-razavi, R. (2017). Improving the thermal shock resistance of thermal barrier coatings through formation of an in situ YSZ/Al 2 O 3 composite via laser cladding. *Journal of Materials Engineering and Performance*, *26*, 1890-1899.
[19] He, B., Zhang, L., Zhu, Q., Wang, J., Yun, X., Luo, J., & Chen, Z. (2020). Effect of solution treated 316L layer fabricated by laser cladding on wear and corrosive wear resistance. *Optics & Laser Technology*, *121*, 105788.
[20] Zhu, L., Xue, P., Lan, Q., Meng, G., Ren, Y., Yang, Z., ... & Liu, Z. (2021). Recent research and development status of laser cladding: A review. *Optics & Laser Technology*, *138*, 106915.
[21] Whitten, J. E. (2001). Blue diode lasers: new opportunities in chemical education. *Journal of Chemical Education*, *78*(8), 1096.
[22] Pasley, J., Andrianaki, G., Baroutsos, A., Batani, D., Benis, E. P., Ciardi, A., ... & Tatarakis, M. (2020). Innovative education and training in high power laser plasmas (PowerLaPs) for plasma physics, high power laser matter interactions and high energy density physics: experimental diagnostics and simulations. *High Power Laser Science and Engineering*, *8*, e5.
[23] Pasley, J., Andrianaki, G., Baroutsos, A., Batani, D., Benis, E. P., Borghesi, M., ... & Tatarakis, M. (2019). Innovative Education and Training in high power laser plasmas (PowerLaPs) for plasma physics, high power laser–matter interactions and high energy density physics–theory and experiments. *High Power Laser Science and Engineering*, *7*, e23.

[24] Senderakova, D., Strba, A., & Mesaros, V. (2008, November). Laser diode module in optical education. In *16th Polish-Slovak-Czech Optical Conference on Wave and Quantum Aspects of Contemporary Optics* (Vol. 7141, pp. 444-450). SPIE.
[25] Keleberda, I. N., Shulika, A. V., Sokol, V. V., Safonov, I. M., Sakalo, T. S., Ivanov, P. S., ... & Lesna, N. S. (2004, July). Web-oriented interactive environment for distance education in study of semiconductor lasers. In *Photonics Applications in Astronomy, Communications, Industry, and High-Energy Physics Experiments II* (Vol. 5484, pp. 561-567). SPIE.
[26] Sabaratnam, A., & Symons, C. (2001, November). Laser entertainment and light shows in education. In *Education and Training in Optics and Photonics* (p. IATLII254). Optica Publishing Group.
[27] Fukuda, M., & Mura, G. (2021). Laser Diode Reliability. In *Advanced Laser Diode Reliability* (pp. 1-49). Elsevier.
[28] Niebauer, T. M., Faller, J. E., Godwin, H. M., Hall, J. L., & Barger, R. L. (1988). Frequency stability measurements on polarization-stabilized He–Ne lasers. Applied optics, 27(7), 1285-1289.
[29] Cheng, W. Y., Chen, Y. S., Cheng, C. Y., Shy, J. T., & Lin, T. (2000). Frequency stabilization and measurements of 543 nm HeNe lasers. *Optical and Quantum Electronics*, *32*, 299-311.
[30] Rowley, W. R. C. (1990). The performance of a longitudinal Zeeman-stabilised He-Ne laser (633 nm) with thermal modulation and control. *Measurement Science and Technology*, *1*(4), 348.
[31] Mohagheghian, M., & Sabouri, S. G. (2018). Laser wavelength measurement based on a digital micromirror device. *IEEE photonics technology letters*, *30*(13), 1186-1189.
[32] Astilean, S., Lalanne, P., Chavel, P., Cambril, E., & Launois, H. (1998). High-efficiency subwavelength diffractive element patterned in a high-refractive-index material for 633?? nm. *Optics letters*, *23*(7), 552-554.
[33] Ara, M. M., Dehghani, Z., Sahraei, R., Daneshfar, A., Javadi, Z., & Divsar, F. (2012). Diffraction patterns and nonlinear optical properties of gold nanoparticles. *Journal of Quantitative Spectroscopy and Radiative Transfer*, *113*(5), 366-372.
[34] Lacraz, A., Theodosiou, A., & Kalli, K. (2016). Femtosecond laser inscribed Bragg grating arrays in long lengths of polymer optical fibres; a route to practical sensing with POF. *Electronics Letters*, *52*(19), 1626-1627.
[35] Liehr, S., Burgmeier, J., Krebber, K., & Schade, W. (2013). Femtosecond laser structuring of polymer optical fibers for backscatter sensing. *Journal of lightwave technology*, *31*(9), 1418-1425.
[36] Jagdeo, J., Nguyen, J. K., Ho, D., Wang, E. B., Austin, E., Mamalis, A., ... & Isseroff, R. R. (2020). Safety of light emitting diode-red light on human skin: Two randomized controlled trials. *Journal of biophotonics*, *13*(3), e201960014.
[37] Li, Y., Zhang, J., Xu, Y., Han, Y., Jiang, B., Huang, L., ... & Qin, C. (2016). The histopathological investigation of red and blue light emitting diode on treating skin wounds in Japanese big-ear white rabbit. *PloS one*, *11*(6), e0157898.